World Conference on
Timber Engineering
Oslo 2023

ANALYTICAL STUDY ON SEISMIC BEHAVIOR OF NEWLY BUILT FIVE STORY PAGODA IN TENDO-CITY JAPAN

Naohito Kawai[1], Mikio Koshihara[2], Iuko Tsuwa[3], Kohei Nakamichi[4]

ABSTRACT: A five story pagoda was built in Tendo-city Japan in 2019 using traditional construction method and structural calculation based on recent technology. First in this paper, the result of micro tremor measurement of the five story pagoda is summarized, next the result of lateral loading test on a shear wall with the same specification of the pagoda is summarized, and finally, the seismic performance of the pagoda is discussed based on the result of time history response analysis using a ten mass system model which is made with considering shear resistance of board walls, rotational resistance of joints between column and penetrating member, *nuki*, and column rocking resistance. As input earthquake waves, we used three artificial waves created with using the response spectrum of extremely rare ground motion stipulated in Building Standard Law of Japan. As the result of the analysis, the pagoda does not collapse even against the strong ground motion though the deformation angle of first story reaches 1/15 radian in some cases.

KEYWORDS: Micro tremor measurement, Time history response analysis, Ten mass system model

1 INTRODUCTION

It is said that there is no historical record that five story pagoda collapsed by earthquake. In the last 100 or so years, many discussions have been made on the seismic performance of five story pagoda in Japan. And even recently, five story pagodas are built using traditional construction method. As one of them, the five story pagoda of *Joan-ji* Temple was built in Tendo-city Japan in 2019 using traditional construction method and structural calculation based on recent technology.

First in this paper, the result of micro tremor measurement of *Joan-ji* five story pagoda is summarized, next the result of lateral loading test on a shear wall with the same specification of the pagoda is summarized, and finally, the seismic performance of the pagoda is discussed based on the result of time history response analysis using the ten mass system model which is made considering the results of the shear wall test.

2 *JOAN-JI* FIVE STORY PAGODA

Figure 1 shows the exterior photograph of the pagoda. Construction of the *Joan-ji* five story pagoda began in 2016 and was completed in August 2019. Height of the pagoda is 32.7 m and the side length of the first floor is 4.62 m.

Species of the structural members is cypress grown in Aomori prefecture. Although traditional construction method is used, engineered structural calculation was made to confirm structural safety according to the current Building Standard Law of Japan.

***Figure 1**: Exterior photograph of the pagoda*

3 MICRO TREMOR MEASUREMENT

3.1 MEASURING METHOD

Figure 2 shows the arrangement of measuring points in the pagoda. Total 14 velocity sensors are placed in sequence on the ground, beams and the center post of the pagoda to cover these 45 measuring points. Time length of one measurement is 500 sec with the sampling frequency 100 Hz. After measuring velocity twice at the same sensor placement we measured displacement also using integrator circuit built into the measuring system.

[1] Naohito Kawai, Kogakuin University, Japan, kawai-nk@cc.kogakuin.ac.jp
[2] Mikio Koshihara, Institute of Industrial Science, The University of Tokyo, Japan, kos@iis.u-tokyo.ac.jp
[3] Iuko Tsuwa, The Japanese Association for Conservation of Architectural Monuments, Japan, tsuwaiuko@gmail.com
[4] Kohei Nakamichi, Tomoe Corporation, Japan, k_nakamichi@tomoe-corporation.co.jp

https://doi.org/10.52202/069179-0335

And after obtaining the values of natural frequencies, we conducted human power excitation at first and second natural frequencies by two persons pushing columns in fifth story for first natural frequency and in third story for second natural frequency, adjusting the pressing time interval to each natural frequency.

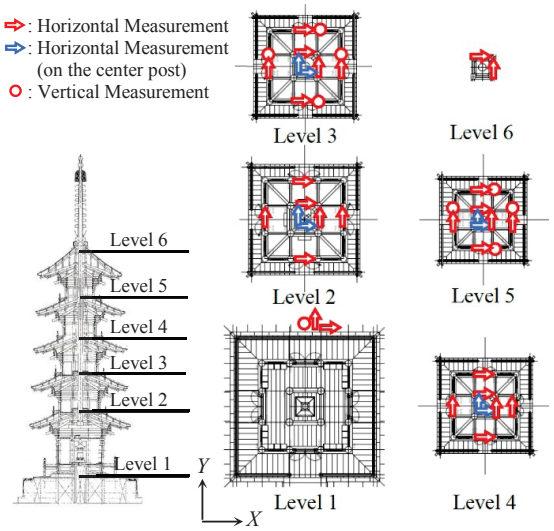

Figure 2: *Arrangement of measuring points*

3.2 RESULT OF MICRO TREMOR MEASUREMENT

By FFT analysis on the measured time history waves, we obtained some values of spectrum peaks. Figure 3 shows the result of FFT analysis. Values of frequency of main spectrum peaks are 1.12 Hz, 3.15 Hz and 5.88 Hz, which are regarded as first to third natural frequencies of the main structure of the pagoda. These observed values are the same in both the X and Y directions.

Figure 4 shows vibration modes in Y direction created by using the ratio of amplitude and the phase difference between measurement points. From Figure 4, we can see that the center column also vibrates with the main structure at first and second natural frequencies. At the third natural frequency, amplitude of the center column is far larger than that of main structure and it is omitted from Figure 4.

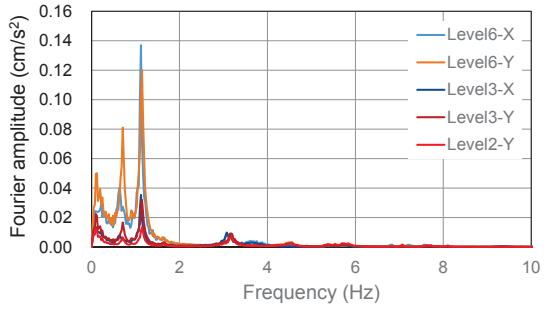

Figure 3: *Result of FFT analysis*

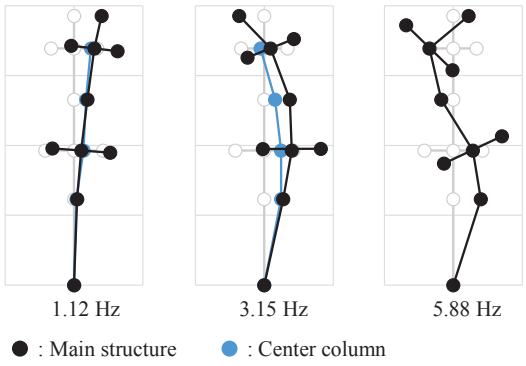

Figure 4: *Vibration mode*

Figure 5 shows the samples of time history waveforms obtained by human power excitation. And Table 1 shows the values of damping ratio at the first and second natural frequencies calculated as the values of logarithmic decrement from the time history waveforms.

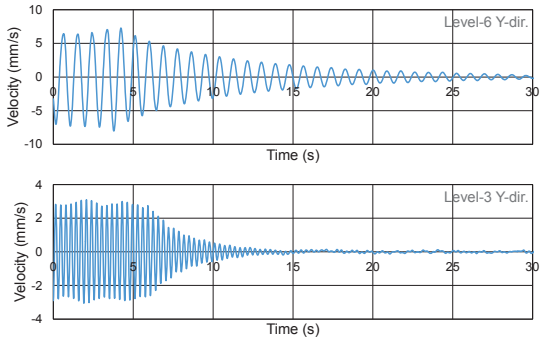

Figure 5: *Samples of time history wave forms obtained by human power excitation*

Table 1: *Values of damping ratio*

Natural frequency (Hz)		Damping ratio (%)
1st	1.12	1.73
2nd	3.15	2.02

4 SHEAR WALL TEST

4.1 TEST SPECIMEN AND TEST METHOD

Figure 6 shows the whole view of the shear wall test, and Figure 7 shows the elevation of the test specimen. The specification of the specimen is same as the wall used in third story of the pagoda.

The species of the members, two column, a sill, a beam and wall boards is cypress. Boards with 50 mm thickness are dropped along the groove of the column and the boards are held together with 9 dowels in each layer. The dowels are made using zelkova. The section of dowels is square of 15 mm by 15 mm, and the length is 120 mm.

https://doi.org/10.52202/069179-0335

The sill of the specimen is fixed by bolts to the base structure and lateral load is applied to the beam using hydraulic actuator.

Lateral cyclic load is applied with 3 cycles at ten target deformation angles, 1/450, 1/300, 1/200, 1/100, 1/75, 1/50, 1/30, 1/20 and 1/15 radians, and finally the displacement reached 123 mm, which is about 1/10 radian in deformation angle.

Figure 6: *Whole view of the shear wall test*

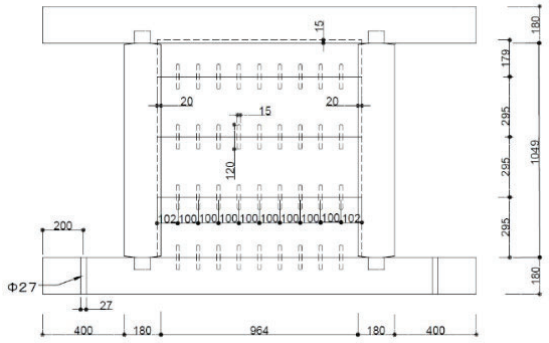

Figure 7: *Elevation of the shear wall specimen (unit: mm)*

4.2 TEST RESULT

Figure 8 shows the load-displacement relationship obtained by the loading test. The load keeps increasing even in a large deformation of 1/10 radian.

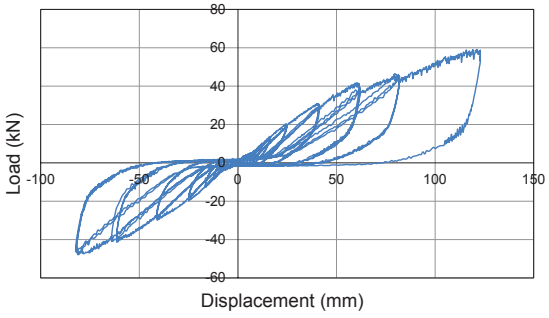

Figure 8: *Load-displacement relationship obtained by the test*

5 TIME HISTORY ANALYSIS

5.1 ANALYSIS METHOD

5.1.1 Overview of the vibration model

Figure 9 shows the concept of ten mass system model and the model for the software "wallstat" [1]. In the model for wallstat, each story consists of two layers. The lower part is is corresponding to the frames and walls and this area deforms by story shear force. The upper part is corresponding to the roof structure and is assumed to be a rigid body. Horizontal resistance of each story is calculated considering shear walls, rotation resistance of joints between column and penetrating member named *nuki* and column rocking resistance. P-Δ effect is also considered as it is built in by default in wallstat. The values of viscous damping is assumed to be 0.02 as instantaneous stiffness proportional type.

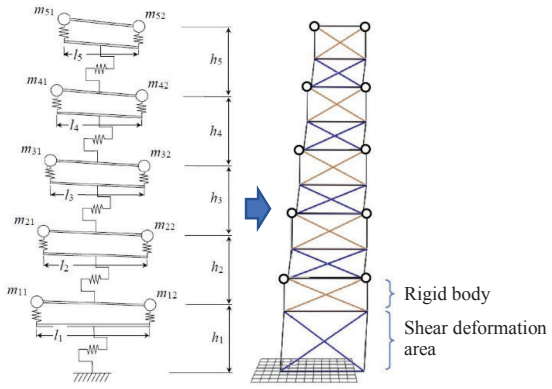

(a) Ten mass system model (b) Model for "wallstat"

Figure 9: *Vibration model*

5.1.2 Values of some parameters

Table 2 shows the values of masses which are obtained by accumulating masses of all the members and roof materials, and values of the length and the height used in the model.

In the roof structure of pagodas, there are some horizontally used timber members and it behaves like vertical springs. The vertical springs are located just below the masses and are assumed to be elastic in this analysis. The value of the spring constant is determined to be 1.81×10^4 kN/m with consulting the result of push over analysis on the three dimensional model which was used in structural calculation in the process of structural design.

Table 2: *Values of masses, length and height in the model*

Story	m_{i1} (ton)	m_{i2} (ton)	L_i (m)	H_i (m)
1st	15.08	15.08	4.62	5.12
2nd	15.21	15.21	4.20	3.65
3rd	13.17	13.17	3.78	3.65
4th	12.19	12.19	3.36	3.65
5th	13.02	13.02	2.94	3.57

https://doi.org/10.52202/069179-0335

5.1.3 Load displacement relationship of shear wall

In order to create the load-deformation relationship of the shear walls in the model, we planned to use theoretical equations for drop board walls given in a guidebook [3], and firstly confirmed the validity between the equations and the experimental results. According to the guidebook, initial stiffness and yield strength of the board wall can be calculated using Equations (1) and (2).

$$K = \frac{1}{\frac{1}{K_a}+\frac{1}{K_b}+\frac{1}{K_c}+\frac{1}{K_d}+\frac{1}{K_s}} \quad (1)$$

where,

K_a = stiffness of the boards as a compression brace,

$$K_a = \frac{E_\theta L t}{2\log\left(L\cos\theta\right)+\frac{1}{\cos^2\theta}-2}$$

K_b = embedment stiffness of the board to the beam,

$$K_b = \frac{L^3 t C_{yb} E_{\perp b}}{15 H d_b}$$

K_c = embedment stiffness of the board to the column,

$$K_c = \frac{aHtC_{yc}E_{\perp c}}{4d_c}$$

K_d = shear stiffness due to dowels,

$$K_d = an_d k_d$$

K_s = shear stiffness of the boards,

$$K_s = GLt$$

$$P_y = \min\left(P_{yd}, P_{ya}\right) \quad (2)$$

where,

P_{yd} = shear strength due to dowels,

$$P_{yd} = n_d \cdot \Delta P_y \left(1+\mu\frac{H}{L}\right)$$

P_{ya} = compression strength when the area of 5% of the diagonal length reaches yield strength,

$$P_{ya} = 0.05Ht\frac{F_\theta}{\sin^2\theta}$$

Parameters L, H, a, t, d_b, d_c, $E_{\perp b}$, $E_{\perp c}$, G, C_{yb}, C_{yc}, n_d, k_d, ΔP_y, μ, θ, E_θ and F_θ for the shear wall test specimen mentioned above are as shown in Table 3.

Figure 10 shows the comparison of load displacement relationship between the calculation result and the test result. The initial stiffness and the yield strength agreed well. As relatively large secondary stiffness was observed in the test result, we assumed secondary stiffness as 35% of the initial stiffness. Moreover, we added first broken point on the relationship of small displacement area to create the proper ratio of bilinear and slip in the hysteresis loop which is built in in the software wallstat as shown in Figure 11.

Table 3: *Values of parameters in Equations (1) and (2) for shear walls in 3rd story*

Symbol	Meaning	Value
L	Inner length of board wall (mm)	964
H	Height of board wall (mm)	1049
a	Board width (mm)	295
t	Board thickness (mm)	50
d_b	Beam height (mm)	180
d_c	Column width (mm)	180
$E_{\perp b}$	Young's modulus perpendicular to the grain of beam (kN/mm^2)	0.3
$E_{\perp c}$	Young's modulus perpendicular to the grain of column (kN/mm^2)	0.3
G	Shear modulus (kN/mm^2)	0.6
C_{yb}	Coefficient of end distance effect of beam	1.8
C_{yc}	Coefficient of end distance effect of column	1.8
n_d	Number of dowels	9
k_d	Shear stiffness of one dowel joint (kN/mm)	1.5
ΔP_y	Shear strength of one dowel joint (kN)	3.8
μ	Coefficient of friction	0.4
θ	Angle of diagonal (rad)	0.828
E_θ	Young's modulus in the direction of diagonal (kN/mm^2)	0.538
F_θ	Compression strength in the direction of diagonal (N/mm^2)	4.78

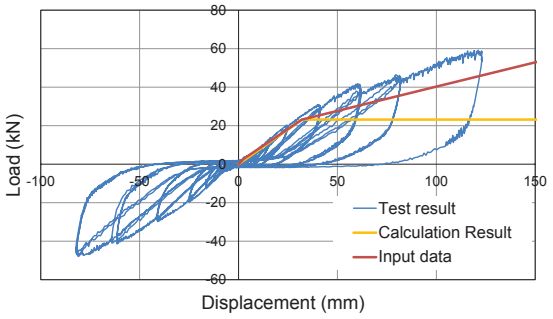

Figure 10: *Comparison of load displacement relationship between calculation result and test result*

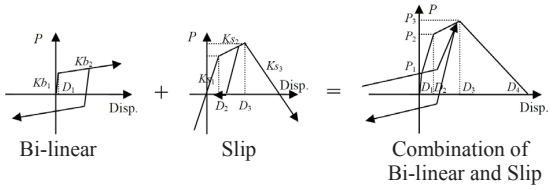

Figure 11: *Hysteresis characteristics of load displacement relationship in the software wallstat* [1]

Thus, we derived load displacement relationship of the shear wall in each story. Table 4 shows the values of parameters in each story. The obtained load value is multiplied by 4 as there located four shear walls in one direction in each story. Table 5 and Figure 12 show the load displacement relationships of the shear deformation

https://doi.org/10.52202/069179-0335

area in each story of the vibration model. The last downward slope after the deformation angle 1/5 radian is a dummy for running the analysis.

Table 4: *Values of parameters in equations (1) and (2) for shear walls in each story*

Story	L (mm)	H (mm)	n_d	θ (rad)	E_θ (kN/mm^2)	F_θ (N/mm^2)
1st	1134	2585	11	1.157	0.355	3.37
2nd	1049	1049	10	0.785	0.581	5.09
3rd	964	1049	9	0.828	0.538	4.78
4th	844	1049	8	0.893	0.484	4.38
5th	724	1049	7	0.967	0.436	4.01

Table 5: *Parameters of load displacement relationship due to shear walls for the shear deformation area*

Story	P1 (kN)	P2 (kN)	P3 (kN)	D1 (mm)	D2 (mm)	D3 (mm)
1st	12.5	103.8	304.6	8.01	100.2	654
2nd	12.8	106.7	446.9	2.58	32.3	326
3rd	11.1	92.5	389.6	2.56	32.1	326
4th	9.1	75.7	317.3	2.58	32.2	326
5th	7.5	62.2	250.2	2.70	33.8	326

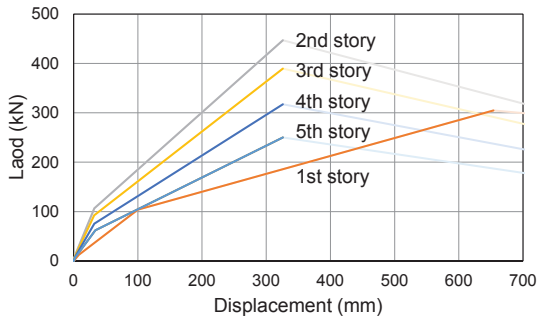

Figure 12: *Load displacement relationship of the shear deformation area in the vibration model due to shear walls*

5.1.4 Load displacement relationship due to rotational resistance of column-*nuki* joint

In order to create the load displacement relationship due to the rotational resistance of column-*nuki* joints, we used theoretical equations given in a design manual [4]. Initial rotational stiffness and yield moment of column-*nuki* joints can be calculated using Equations (3) and (4).

$$K_{\theta b} = {x_p}^2 y_p E_\perp \left\{ \frac{x_p}{Z_0}\left(C_{xm} - \frac{1}{3} \right) + 0.5\mu C_{xm} \right\} \quad (3)$$

$$M_{yb} = \frac{K_{\theta b} Z_0 F_m}{x_p E_\perp C_{xm} \sqrt{C_{ym}}} \quad (4)$$

where,

F_m = Embedment yield stress when end and edge distances are infinite

$$F_m \simeq \frac{2.4}{3} F_{cv}$$

F_{cv}: Embedment strength, F_{cv} = 7.8 (N/mm^2)

C_{xm}: Coefficient of end distance effect in length direction of *nuki*

$$C_{xm} = 1 + \frac{4Z_0}{3x_p}$$

C_{ym}: Coefficient of edge distance effect in width direction of *nuki*

$$C_{ym} = 1 + \frac{4Z_0}{3ny_p}$$

Table 6 shows the meaning of symbols, x_p, y_p, Z_0, $E_\perp$, n *and* μ, and Table 7 shows the values in each story. And Table 8 shows the calculated values of initial rotational stiffness $K_{\theta b}$ and yield moment M_{yb} in each story and of each column diameter.

Table 6: *Meaning of symbols in Equations (3) and (4)*

Symbol	Meaning
x_p	Half of column width or diameter (mm)
y_p	Width of *nuki* (mm)
Z_0	Height of *nuki* (mm)
$E_\perp$	Young's modulus perpendicular to grain of *nuki* (kN/mm^2)
n	Replacement factor of X and Y directions
μ	Coefficient of friction

Table 7: *Values of parameters in each story*

Symbol	Story	Value
x_p (mm)	5th story*1	150, 130
	4th story*1	160, 140
	3rd story*1	170, 150
	2nd story*1	180, 160
	1st story*1	190, 170
y_p (mm)	2nd to 5th story	115
	1st story	100
Z_0 (mm)	2nd to 5th story	175
	1st story	210
$E_\perp$ (kN/mm^2)		0.18
n		6
μ		0.8

*1: First is x_p of inner column and second is of outer column.

Table 8: *Values of initial rotational stiffness and yield moment in each story*

Story	x_p (mm)	Number of joints	$K_{\theta b}$ (kNm/rad)	M_{yb} (kNm)
1st	190	4	3026	25.19
	170	8	2251	10.94
2nd	180	4	2672	25.70
	160	8	1948	21.08
3rd	170	4	2291	23.34
	150	8	1640	18.94
4th	160	4	1948	21.08
	140	8	1367	16.90
5th	150	4	1640	18.94
	130	8	1124	14.98

https://doi.org/10.52202/069179-0335

To create the load displacement relationships due to the rotational resistance of column-*nuki* joints in each story, the load is calculated as the summation of moment of joints divided by the height of shear deformation area of the vibration model, and the displacement is calculated as the product of height of shear deformation area and rotation angle of joint. Though the diameter of column differs between the inner column and outer column in the same story, the difference of the rotation angle of yield point is small. Therefore, we used the summation of the initial stiffness and the summation of the yield moment in each story to derive the load displacement relationship of shear deformation area of each story.

Moreover, it is known that the relationship of moment and rotation angle of these joints has a relatively large secondary stiffness, so we assumed secondary stiffness of 1/12 of initial stiffness with reference to the result of the preceding study [5]. And we added first broken point on the relationship of small displacement area to create the proper ratio of bilinear and slip in the hysteresis loop.

Table 9 and Figure 13 show the load displacement relationships due to the rotational resistance of column-*nuki* joints in each story used in the shear deformation area of the vibration model. The last downward slope after the deformation angle 1/5 radian is a dummy for running the analysis.

Table 9: *Parameters of load displacement relationship for the shear deformation area in each story of the vibration model*

Story	P1 (kN)	P2 (kN)	P3 (kN)	D1 (mm)	D2 (mm)	D3 (mm)
1st	8.2	82.1	228.7	1.46	29.1	654
2nd	16.7	166.5	421.3	0.84	16.8	326
3rd	15.0	150.2	365.6	0.90	17.9	326
4th	13.5	134.7	314.9	0.96	19.1	326
5th	12.0	120.0	269.0	1.02	20.5	326

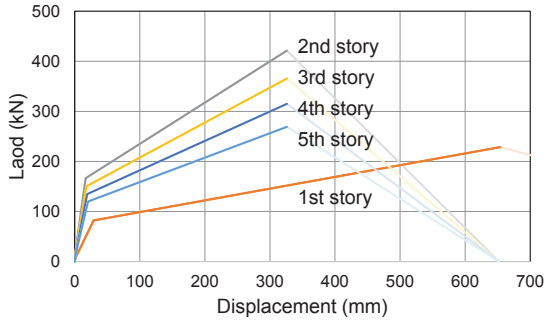

Figure 13: *Load displacement relationship of the shear deformation area due to rotational resistance of column-nuki joints*

5.1.5 Column rocking resistance

When a thick column tilts by lateral load, vertical load on the column works to reduce the tilting angle. This effect is called column rocking resistance and is one of the important seismic element of traditional timber buildings [6]. The function is built into the software wallstat to add column rocking resistance as the moment at the bottom of column.

Table 10 shows the parameters input to the vibration model. There are two columns in each story in the model, the values of vertical load in Table 10 are that of one column. And the values of vertical load from 2nd to 5th stories are decreased to 5/8 of the original values as these columns are surrounded by wood on top and bottom and the effect is smaller than the column on foundation stone.

Figure 14 shows the load displacement relationship due to column rocking resistance calculated by Equation (5), which is based on the equation originally derived from the experiment result on circular section column by Ban [7], but does not contain the P-Δ effect as the P-Δ effect is considered for the whole model in the software wallstat.

$$P_c = \frac{b}{h} W \left(1 + 0.99625 e^{-0.03027\delta} - \frac{19.9625}{\delta + 10} \right) \qquad (5)$$

where, P_c = lateral load due to column rocking resistance (kN), b = column diameter (mm), h = column height (mm), W = vertical load (kN) and δ = displacement (mm).

Table 10: *Parameters of column rocking resistance of one column in the vibration model*

Story	Column diameter b (mm)	Column height h (mm)	Vertical load W (kN)
1st	340	3270	673.4
2nd	320	1630	328.5
3rd	300	1630	235.3
4th	280	1630	154.5
5th	260	1630	79.8

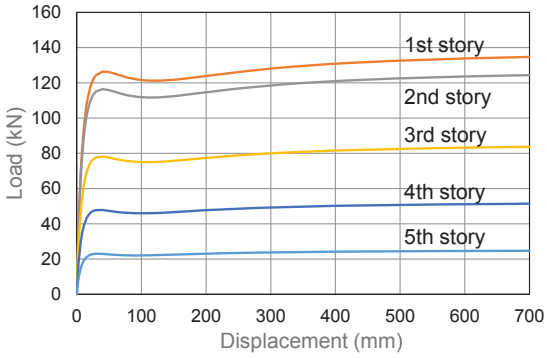

Figure 14: *Load displacement relationship of the shear deformation area due to column rocking resistance*

5.2 INPUT EARTHQUAKE WAVE

As the input earthquake waves, we used three artificial waves created with using the response spectrum of extremely rare ground motion stipulated in Building Standard Law of Japan. Figure 15 shows the acceleration response spectrum and Figure 16 shows the time history of acceleration of these waves.

https://doi.org/10.52202/069179-0335

Hachinohe-NS is created using an amplification factor of acceleration by surface ground G_s calculated by the boring data near the site and the phase spectrum of the observed wave at Hachinohe during the Tokachi-oki earthquake in 1968. Tendo-EW is also created using the boring data and the phase spectrum of the observed wave at Tendo during the 2011 off the Pacific coast of Tohoku earthquake. BSL1 is using G_s of type 1 ground stipulated in Building Standard Law of Japan and a random phase spectrum.

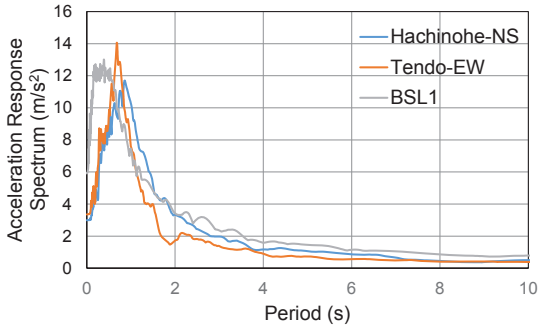

Figure 15: *Acceleration response spectrum of input waves*

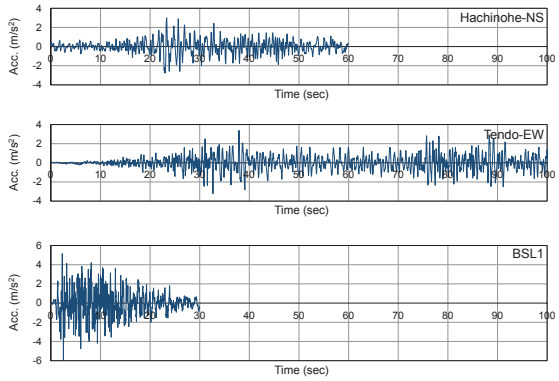

Figure 16: *Time history of acceleration of input waves*

5.3 ANALYSIS RESULT

As an example of the result of time history analysis, Figures 17 and 18 show the time history waveform of story drift and the relationships between story shear force and story drift, against the input wave using Hachinohe-NS phase. Table 11 and Table 12 show the maximum values of story drift δ_{max} and shear deformation angle γ_{max} against each input wave.

From Table 11 and Table 12 we can see that the maximum story drift of first story is far larger than other stories and it reaches 342.7 mm against BSL1, which is about 1/15 radian by story shear deformation angle. However, the pagoda does not collapse against the strong ground motion according to the requirement of Building Standard Law of Japan.

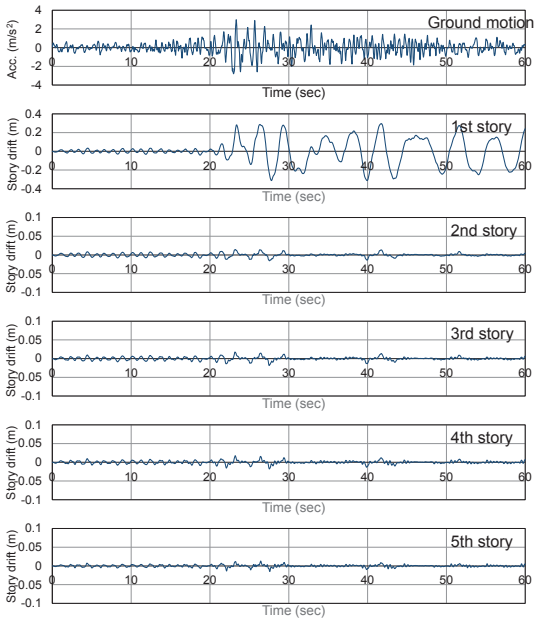

Figure 17: *Time history of story drift against Hachinohe-NS as an example of the analysis result*

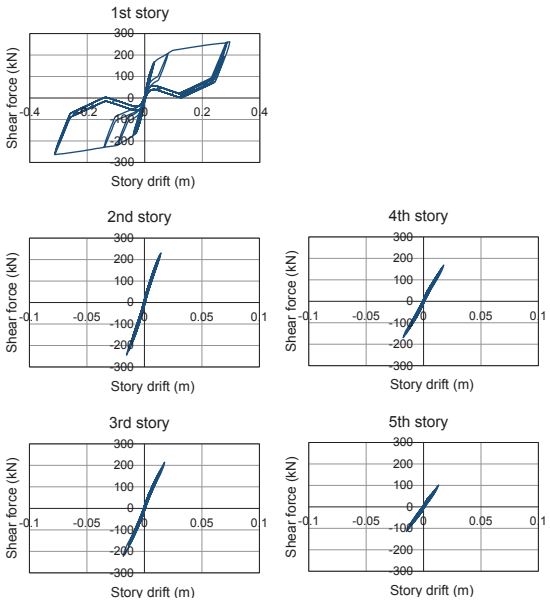

Figure 18: *Relationship between story shear force and story drift against Hachinohe-NS as an example of the analysis result*

Table 11: *Maximum values of story drift δ_{max} (mm)*

Story	Story drift δ_{max} (mm)		
	Input waves		
	Hachinohe-NS	Tendo-EW	BSL1
1st	312.9	295.0	336.5
2nd	15.6	16.3	15.8
3rd	18.4	18.9	16.3
4th	17.8	19.1	15.8
5th	15.0	15.0	15.1

https://doi.org/10.52202/069179-0335

Table 12: *Maximum values of shear deformation angle γ_{max}*

Story	Shear deformation angle γ_{max} (10^{-3} rad)		
	Input waves		
	Hachinohe-NS	Tendo-EW	BSL1
1st	61.1	57.6	65.7
2nd	4.3	4.5	4.3
3rd	5.0	5.2	4.5
4th	4.9	5.2	4.3
5th	4.1	4.1	4.1

In this analysis, only the main seismic elements are considered but there are other structural element that can be considered such as rotational resistance of many other joints. Especially, the ratio of shear stiffness of first story to other stories seems smaller considering the result of microtremor measurement. Therefore, actual maximum displacement may smaller than this analysis result and further study for more appropriate modeling seems necessary.

6 CONCLUSIONS

We conducted micro tremor measurement and performed time history response analysis on the newly built five story pagoda of *Joan-ji* temple in Tendo-city Japan. As the result of micro tremor measurement, we obtained natural frequencies and vibration modes. And the result of the time history analysis considering shear resistance of board walls, rotational resistance of the joints between column and *nuki*, and column rocking resistance, clarified that the pagoda does not collapse against the strong ground motion at the level of the requirement of standard though the deformation angle of first story reaches 1/15 radian in some cases.

ACKNOWLEDGMENT

Authors would like to thank Mr. Yasuo Matsuoka, the chief priest of *Joan-ji* Temple, for his full cooperation in this research, Dr. Takafumi Nakagawa, Associate Professor of Kyoto University, for his advice to use the analysis software wallstat, Mr. Takahiro Sato, who designed the structure of the pagoda, for his provision of technical data and all the members of Kawai laboratory in Kogakuin University who assisted with experiments, measurements and so on.

REFERENCES

[1] T. Nakagawa, M. Ohta, et. al.: Collapsing process simulations of timber structures under dynamic loading III Numerical simulations of the real size wooden houses, Journal of Wood Science, Vol.56, No.4, 284-292, 2010.

[2] A. Kuramoto, N. Kawai, et. al.: Analytical study on seismic performances of a newly built five-storied pagoda, Proceedings of WCTE 2018, 2018.

[3] Technical guidebook on wall multiplying factors for clay walls, lattice walls, and drop board walls (in Japanese), HOWTEC, 2004.

[4] Design manual for engineered timber joints (in Japanese), Architectural Institute of Japan, 2009.

[5] S. Murai and M. Miyamoto: Experimental study on structural performance evaluation of column-to-*nuki* connection in traditional timber shrines and temples, AIJ Journal of Technology and Design, Vol. 27, No.66, 714-719, 2021.

[6] N. Kawai: Static loading test and shake table test on column rocking resistance using scale models, Proceedings of WCTE 2018, 2018.

[7] S. Ban: Study of statics on structure of temples and shrines Part 1 (in Japanese). Technical papers of annual meeting, Architectural Institute of Japan, 1941.

https://doi.org/10.52202/069179-0335